ELSEVIER

Journal of Molecular Catalysis A: Chemical 161 (2000) 179–189

JOURNAL OF MOLECULAR CATALYSIS A: CHEMICAL

www.elsevier.com/locate/molcata

A general model for both three-way and deNO$_x$ catalysis: dissociative or associative nitric oxide adsorption, and its assisted decomposition in the presence of a reductant
Part I. Nitric oxide decomposition assisted by CO over reduced or oxidized rhodium species supported on ceria

Gérald Djéga-Mariadassou [a,*], Franck Fajardie [b], Jean-François Tempère [a], Jean-Marie Manoli [a], Olivier Touret [c], Gilbert Blanchard [b]

[a] *Laboratoire Réactivité de Surface, Université Pierre et Marie Curie, CNRS UMR 7609, Case 178, 4 Place Jussieu 75252, Paris Cedex 05, France*

[b] *Rhodia Recherches, 52 Rue de la Haie Coq, 93308 Aubervilliers Cedex, France*

[c] *Rhodia, Chimie Secteur I.O.M. Usine de La Rochelle B.P. 2049, 17010 La Rochelle Cedex, France*

Received 18 October 1999; received in revised form 10 February 2000; accepted 6 June 2000

Abstract

A selective overview of recent studies on both three-way and deNO$_x$ catalysis (we shall note 'deNO$_x$', the removal of NO in the presence of an excess of oxygen) leads to an unique and general model of these reactions, based on kinetic concepts. Two kinds of active sites have to be first defined: cationic and zero-valent metal ones.

The first type can form either through the reduction of the support ($_V$)-Ce^{3+}-($_V$) or (ii) a strong metal-support interaction ($_V$)-Rh^{+}-($_V$)/CeO_2, both linked to adjacent oxygen vacancies ($_V$) of the reducible support, or (iii) a surface transition metal (TM) complex (TM in zeolite for instance). The second kind of sites are accessible supported-zero-valent noble metal atoms. These two kinds of sites are involved in three-way Catalysts (TWC), whereas only the cationic ones concern deNO$_x$ reactions. Therefore, nitric oxide chemisorption can be either 'associative' on the first kind of sites — leading to dinitrosyl or hyponitrite species — or 'dissociative', on the second ones, leading to oxygen and nitrogen atoms adsorbed on the sites. Two different catalytic sequences of elementary steps can then be defined. On cationic sites, successive N–O bond scissions of dinitrosyl or hyponitrite species occur, potentially able to produce intermediate N_2O, and in all cases leaving oxygen atoms adsorbed on the active site, and inhibiting a further adsorption of NO. A reductant is then necessary to remove these oxygen atoms and permit the reaction to proceed further. On zero-valent metallic sites, at the temperature of reaction, NO suffers a dissociative chemisorption leading again to surface oxygen atoms. Again, a reductant is necessary to remove these oxygen species and permit the reaction to proceed again. In this first paper, TWC are considered and the reductant is CO.

* Corresponding author. Tel.: +33-144-27-36-26; fax: +33-144-27-36-26.
E-mail address: djega@moka.ccr.jussieu.fr (G. Djéga-Mariadassou).

1381-1169/00/$ - see front matter © 2000 Elsevier Science B.V. All rights reserved.
PII: S1381-1169(00)00334-4

Two catalytic cycles are considered based on our results on temperature-programmed desorption and surface reactions of NO in a stoichiometric $CO/NO/O_2$ mixture. © 2000 Elsevier Science B.V. All rights reserved.

Keywords: Associative/Dissociative NO chemisorption; Assisted catalysis; General model; Rhodium

1. Introduction

The global reduction of nitric oxide to dinitrogen in the presence of carbon monoxide still remain a catalytic reaction of great interest in pollution abatement, especially in view of studying three-way catalysts (TWC) in lean-burn conditions (green house effect and storage and release processes).

One of the general remarks of Pârvulescu et al. [1], in their recent extensive review on catalytic removal of NO, is that 'in spite of the tremendous work done in this field, the best solution for removal of NO has still not been found'. Nevertheless, it appears to the present authors that a general understanding of both three-way and $deNO_x$ catalysis (we shall note '$deNO_x$', the removal of NO in the presence of an excess of oxygen), through a selective approach of the already published data, can help to solve the problem of the best catalyst for removal of NO in car exhaust.

Three-way and $deNO_x$ catalysis follow the same general catalytic sequence: NO decomposes on the active site, leading to N_2 and O(ads), and the reaction is then controlled by the oxygen-scavenging process through a reaction between the adsorbed reactant and O(ads). Depending on the catalytic process (TWC or $deNO_x$) the nature of the active site varies, as well as the reductant. The N-containing reactive intermediates are either NO(ads), or dinitrosyl groups, or hyponitrites.

The very important and interesting point in both TWC and $deNO_x$ processes is the simultaneous activation of NO(ads) and reductant(ads) as evidenced by transient temperature programmed reactions, leading to the 'assisted' reduction of NO by this reductant. We never have a direct interaction between NO and the reductant, but rather two main steps: decomposition of NO and oxygen-scavenging by the reductant.

In agreement with Burch and Millington [2], we think that not too much significance should be attached to carbonaceous deposits (formed at the surface of acidic supports), for the conversion of nitrogen monoxide into dinitrogen, in lean burn conditions ($deNO_x$), these deposits being rather considered as stable spectator species in large quantities at the surface of the catalyst.

In the work reported here, we first investigate the NO decomposition over Rh/CeO_2 with CO as a reductant, for stoichiometric conditions. The role of ceria in three-way catalysis will be included in the mechanistic model. First, the general features of the model will be defined, then we shall discuss how our experimental data upon temperature-programmed surface reactions (TPSR) will enter the general framework. One characteristics of our experimental work, is the continuous analysis of reactants at the reactor outlet (equivalent to a continuous stirred reactor), using specific detectors: it permitted us to evidence the detailed sequence of elementary steps of the 'assisted' reduction of NO in the presence of CO during TPSR and therefore, to propose two coupled catalytic cycles for TWC over a reduced metal M(0), and a catalytic cycle over an oxidized metal both cycles leading to an unified kinetic model from TWC (stoichiometric $CO/NO/O_2$ mixture) to $deNO_x$ (lean conditions).

2. Experimental and theoretical basis of the model

2.1. Reduced or oxidized precious metal

As a result of previous extensive researches, the reaction mechanism for the global reduction of NO by CO ($2NO + 2CO = N_2 + 2CO_2$) on Pt or Rh catalysts seems to be reasonably understood [3–8] as far as precious metals are reduced.

However, there has been some controversy regarding the oxidation state of rhodium, some authors assuming this precious metal to be oxidized during the catalytic cycle [9,10]. Hyde et al. [10] considered individual rhodium atom sites or edge sites with cationic character due to some interactions between metal atoms and the support. Chuang and co-workers [11–13] on Rh/SiO_2, starting from Rh(0), considered that the 'reduction of NO by CO' goes through

the oxidation of Rh(0) to Rh^+ at the surface of the precious metal: then Rh^+ can chemisorb NO. Fajardie et al. [14] found CeO_2–ZrO_2 able to stabilize 100% rhodium as Rh^{x+} (with x probably equal to 1) into Ce^{4+} vacancies of the support.

2.2. Dissociative chemisorption of nitric oxide over reduced precious metals

Previous studies on NO chemisorption over TWC lead to some clear conclusions on the nature of NO adsorption. Burch et al. [15] found that nitric oxide dissociates on *reduced* platinum sites. Root et al. [6] found that NO on Rh(1 1 1) dissociates between 273 and 323 K. Leclercq et al. [16], Cho et al. [9] also assumed NO dissociation through two elementary steps over *reduced* Pt or Rh

$$NO + * \rightleftarrows {}^*NO$$
$${}^*NO + * \rightleftarrows {}^*N + {}^*O$$

where (*) is a zero-valent metal atom.

Kaspar et al. [17] have shown that, in the presence of agglomerated particles, both NO dissociation and adsorbed N are promoted. Hecker and Bell [18] rationalized their results in a reaction sequence in which the above two steps are included.

In quantum mechanic computation using extended Hückel methods, Ward et al. [19] studied the interaction between NO and Rh(1 0 0), Pt(1 0 0) and Pd(1 0 0) as models. One of their main conclusions was that the dissociative chemisorption of NO is favored by the Rh surface as a consequence of compatibility between the Fermi level of the metal with that of the adsorbed NO.

The first important conclusion of these previous studies (we cite only a few) is that in the presence of Pt(0) or Rh(0), NO dissociates into N(ads) and O(ads), even at 273 K. In what follows, we shall refer to this process as a 'dissociative chemisorption of NO'.

2.3. Associative chemisorption of NO and CO over oxidized precious metals

On the contrary, in the presence of oxidized rhodium surface species, we shall have to consider an 'associative chemisorption of NO' on the active sites. Arai and Tominaya [4] studied Rh/Al_2O_3. They found, by infrared spectrometry, that NO adsorbs without any dissociation and leads to complexes similar to $Rh(CO)(NO)(PPh_3)$ taken as a reference.

Iizuka and Lunsford [22] in 1980, concluded that at temperatures less than 470 K, rhodium ions in Y-Zeolite are active for the reduction of NO by CO, but the reaction mainly formed N_2O. The $[Rh^I(CO)_2NO]^+$ complex was proposed as an intermediate in the catalytic reaction. Both $[Rh^I(CO)_2]^+$ and $[Rh^I(NO)_2]^+$ complexes were also observed over the Rh/Y-Zeolite. This is a very nice example, similar to homogeneous catalysis, of identification of Rh^I complexes, where NO and CO are ligands in the coordinative sphere of rhodium(I). In solution chemistry, Hendriksen et al. [23] have proposed that $[Rh^I(Cl)_2(CO)_2]^-$ reacts with NO, forming $[Rh^{III}(Cl)_2(CO)(NO^-)_2]^-$ which was believed to be a catalytic intermediate in the reaction ($2NO + CO = N_2O + CO_2$). Salin [24] has studied NO adsorption/desorption on commercial but simplified three-way catalysts (Pt alone, Pd alone or Rh alone on CeO_2–ZrO_2–Al_2O_3/ honeycomb materials); this author has found that a fraction of NO adsorbed at room temperature always desorbed at the temperature of the reaction $CO/NO/O_2$ (for stoichiometric mixture), clearly evidencing that a fraction of the precious metal should be in an oxidized state. Furthermore, this result shows that it is always very difficult to completely reduce supported precious metals, probably due to very strong metal-support interactions. This result can also explain data from literature assuming the existence of oxidized transition metal atoms on materials globally considered as reduced catalysts [4].

Fajardie et al. [14] have assumed the formation of $Rh^{x+}(NO)_2$ surface species (dinitrosyl) over CeO_2–ZrO_2 and evidenced a NO:Rh ratio equal to 2:1. Rh was dispersed as isolated ions on the support and unable to hydrogenate benzene, a molecular probe for testing the presence of reduced Rh [25].

Finally, Soria et al. [26,27] have shown that hyponitrites can form on ceria by adsorption of two NO molecules close to [Ce^{3+}-oxygen vacancy] sites, as follows

$$2\left[Ce^{3+}\text{-}(_V)\right] + 2NO = Ce^{4+}\text{–}[ONNO]^{2-}\text{–}Ce^{4+}$$

The *cis*-hyponitrite species has been observed by infrared spectroscopy whereas N_2O adsorbed and in the gas phase have been detected [26]. Furthermore,

NO did not dissociate on Ce^{4+} sites, and was able to desorb from ceria surface during temperature programmed desorption (TPD) experiments [27].

Carbon monoxide, the reductant, also plays the role of ligand on these oxidized rhodium supported catalysts. Primet [28] in an infrared study of CO chemisorption on zeolite and alumina supported rhodium, have evidenced that adsorption of CO leads to the formation of *gem*-dicarbonyl species of oxidized rhodium, probably in the Rh^{I} state. $Rh^{+}(CO)_2$ was the main species observed over RhNaY.

Chuang et al. [11–13] also considered that Rh^{+} can chemisorb either NO or *gem*-dicarbonyl $Rh^{+}(CO)_2$. We already saw that Arai and Tominaga [4] compared the species detected by infrared spectroscopy over Rh/SiO_2 to $Rh(CO)(NO)(PPh_3)_2$.

2.4. N_2O as an intermediate of the $CO/NO/O_2$ reaction

There has been also another controversy regarding N_2O formation during NO decomposition or (CO/NO) reaction on Rh catalysts [9]. Rhodium particle size effect [20] and nature of single crystal face exposed to the reaction have been also studied. Campbell and White [5] and Root et al. [6] did not observe the formation of N_2O neither on powder of Rh nor on Rh(1 1 1), whereas Castner and Somorjai [21] observed a significant amount of N_2O on Rh(S)-[6(1 1 1) × (1 0 0)].

N_2O is generally considered to form over Pt(0) or Rh(0). Cho et al. [9] as well as Hecker and Bell [18] have proposed the following two steps:

$$^{*}NO + * \rightarrow {}^{*}N + {}^{*}O$$

$$^{*}NO + {}^{*}N \rightarrow N_2O + 2*$$

where $(*)$ stands for a reduced metallic site.

Over cationic sites, Soria et al. [26,27] assumed that hyponitrites can lead to the desorption of N_2O from the surface of ceria. Fajardie et al. [14] detected very low amount of N_2O in the gas phase during transient experiments over $Rh/CeO_2–ZrO_2$ system and more previously, Iizuka and Lunsford [22] only observed N_2O formation over Rh/Y-zeolite in the presence of CO.

Table 1
Network of reactions over reduced noble metals[a]

	Reactions	σ_1	σ_2	σ_3	σ_4
(1)	$O_2 + * \rightleftarrows {}^{*}O\,{}^{*}O$	0	1	0	0
(2)	$O\,{}^{*}O + * \rightleftarrows 2\,{}^{*}O$	0	1	0	0
(3)	$NO + * \rightleftarrows {}^{*}NO$	2	0	2	2
(4)	$^{*}NO + * \rightleftarrows {}^{*}N + {}^{*}O$	1.5	0	1	2
(5)	$^{*}N + {}^{*}N \rightleftarrows N_2 + 2*$	0.5	0	0	1
(6)	$CO + * \rightleftarrows {}^{*}CO$	2	2	1	2
(7)	$^{*}CO + {}^{*}O \rightleftarrows CO_2 + 2*$	2	2	1	2
(8)	$^{*}N + {}^{*}NO \rightleftarrows {}^{*}N_2O + *$	0.5	0	1	0
(9)	$^{*}N_2O \rightleftarrows N_2O + *$	0	0	1	0
(10)	$^{*}N_2O \rightleftarrows N_2 + {}^{*}O$	0.5	0	0	0
R(1)	$2NO + 2CO = N_2 + 2CO_2$				
R(2)	$2CO + O_2 = 2CO_2$				
R(3)	$2NO + CO = N_2O + CO_2$				
R(4)	$2NO + 2CO = N_2 + 2CO_2$				

[a] σ_i are stoichiometric numbers and R(i) the different reaction route without $^{*}N_2O$ species (see Fig. 2).

2.5. Sequence of elementary steps for the reduction of NO in the presence of CO and O_2 (for stoichiometric mixture)

The overview of literature only leads to a well defined sequence over reduced noble metals. On the contrary, only few data have been published for the $CO/NO/O_2$ reactions over oxidized rhodium or platinum.

2.5.1. Elementary steps over reduced precious metals

Considering data from Hecker and Bell [18], Cho et al. [9], Harrison et al. [29], Leclercq et al. [16] and Burch et al. [30] using TAP (temporal analysis of products) experiments, we can summarize the various elementary steps in the network of reactions [31] (Table 1).

2.5.2. Elementary steps over supported oxidized Rh

The first pathway proposed by Iizuka and Lunsford [22] concerns the reduction of nitric oxide by CO over rhodium-Y-zeolite. It leads only to N_2O as follows

$$Rh^{I}(CO)_2 + NO \rightleftarrows Rh^{I}(CO)_2(NO)$$

$$Rh^{I}(CO)_2(NO) + NO \rightleftarrows Rh^{I}(CO)\text{-}(_V) + N_2O + CO_2$$

where ($_V$) is an oxygen vacancy in the coordinative sphere of the metal. Complexes such as $Rh^I(CO)(NO)$ and $Rh^I(NO)_2$ were also considered. In solution chemistry, Hendriksen et al. [23] assumed that the following sequence can occur, leading to N_2O formation:

$$Rh^I(CO)_2 + 2NO \rightleftarrows Rh^{III}(CO)(NO^-)_2 + CO$$

$$Rh^{III}(CO)(NO^-)_2 \rightleftarrows Rh^I + N_2O + CO_2$$

Cataluna et al. [27] also proposed the formation of N_2O over ceria alone as follows:

$$2\left[Ce^{3+}\text{-}(_V)\right] + 2NO \rightleftarrows Ce^{4+}\text{–}(ONNO)^{2-}\text{–}Ce^{4+}$$

$$Ce^{4+}\text{–}(ONNO)^{2-}\text{–}Ce^{4+} \rightleftarrows (Ce^{4+}\text{–}O^{2-}) + \left[Ce^{4+}\text{-}(_V)\right] + N_2O$$

where ($_V$) stands for an oxygen-vacancy of ceria.

As a summary, we can list the main features which have to be taken into account at the basis of our model.

1. There are two possible kinds of sites over three-way catalysts: *reduced* precious metals and *oxidized* ones.
2. NO suffers a *dissociative* chemisorption over reduced sites.
3. NO suffers an *associative* chemisorption over oxidized sites, leading to dinitrosyl or hyponitrite species.
4. The sequence of elementary steps over reduced sites is reasonably understood and leads to a network of three catalytic routes: NO decomposition assisted by CO; CO oxidation to CO_2 alone; N_2O formation.
5. No complete catalytic sequence has been proposed till now for $CO/NO/O_2$ reactions over oxidized rhodium leading to ($N_2 + CO_2$).
6. Ceria is able to promote the NO reduction to N_2O.
7. NO has been observed to desorb (TPD experiments) from ceria, indicating the lack of dissociation over oxidized noble metal sites.

On these basis, and considering our TPSR experiments for $CO/NO/O_2$ reactions over ceria, we shall establish two feasible catalytic cycles for these reactions, depending on the nature of the active site, and taking into account all the preceding features.

3. Experimental

3.1. Catalyst preparation

Two kinds of Rh/CeO_2 were prepared: the first one only containing Rh(0) accessible atoms owing to a pre-sintering of the support, avoiding strong metal-support interactions due to the low surface area; the second one containing both Rh(0) and Rh^{x+}, prepared on high surface area ceria.

Pure ceria with high specific surface area (HS) (141 $m^2\,g^{-1}$) was provided by Rhodia and used as support, either as received and noted CeO_2 HS, or after calcination at 1173 K with a low surface area (LS) (6 $m^2\,g^{-1}$) and noted CeO_2 LS. Ceria containing rhodium samples were obtained by anionic exchange at low pH (1.9) using $RhCl_3$ solution according to a method described elsewhere [14]. Rh exchange was conducted both on the high and low surface area ceria, leading, respectively, to the Rh/CeO_2 HS and Rh/CeO_2 LS samples with 0.31 and 0.15 wt.% rhodium, respectively.

3.2. Catalyst characterization

Specific surface areas of bare HS and LS ceria and ceria supported rhodium were determined using the BET method and a Quantasorb Jr. Dynamic system.

Counting of Rh(0) species using an insensitive structure reaction [31]. Benzene hydrogenation measurements were conducted in a conventional device described elsewhere [25,32]. In a typical run, prior to benzene hydrogenation, catalysts were pretreated at 773 K in flowing hydrogen, then cooled to the temperature of reaction under helium, and finally submitted to the H_2/C_6H_6 mixture. It has been shown [25,32] that the number of exposed zero-valent Rh(0) atoms (active sites) can be deduced from the turnover rate (V_r) [31]

$$V_r\,(s^{-1}) = \frac{\text{reaction rate}\,(\text{mol}\,C_6H_6\,s^{-1}\,g^{-1})}{\text{number of active sites}\,(\text{mol}\,g^{-1})}$$

$CO/NO/O_2$ reactions were performed at atmospheric pressure in a dynamic flow reactor using the

same experimental conditions as used in a previous work [14]. All catalytic runs were performed after a pretreatment of catalysts in flowing hydrogen at 773 K. The catalytic activities of the samples were characterized in the $CO/NO/O_2$ reactions in temperature programmed experiments from 298 to 773 K (light-off conditions) at a constant heating rate of 453 K h^{-1} with a space velocity from 90 to 125,000 h^{-1}. The feed stream (15 l h^{-1}) consisted of a stoichiometric gas mixture containing 1.5 vol.% CO, 0.20 vol.% NO, and 0.65 vol.% O_2 in helium, the composition of which being monitored by mass flowmeters. The catalyst sample (200 mg) was placed in an oven whose heating rate was monitored by a West 2050 programmator. In these conditions, the reactor behaves like a continuous stirred reactor (CSTR). Continuous analysis of the gas mixture at the inlet and at the outlet of the reactor was performed by a Maihak Finor infrared detector for CO, a Thermoelectron chemiluminescent NO/NO_x analyzer for NO, and by gas chromatography to control the eventual presence of N_2O in the effluents. Experimental data were given as conversion versus temperature plots allowing the determination of the temperature of light-off (50% conversion) of reactants.

Counting of Rh^{x+} species active in the $CO/NO/O_2$ reactions was proceeded according to the so called 'NO adsorption–desorption method' [14] consisting in the evaluation of the number of undissociated NO molecules desorbing at the light-off temperature of the CO/O_2 reaction, and assuming a NO:Rh ratio equal to 2:1. Prior to each thermodesorption, fresh samples were activated up to 773 K using a 1.5 vol.% CO/0.65 vol.% O_2 in helium (15 l h^{-1}) as reducing mixture. Then adsorption of NO in helium on the activated catalyst was carried out at room temperature using a 0.2 vol.% NO in He (15 l h^{-1}). Finally thermodesorption of adsorbed NO, in the CO/O_2/He mixture was conducted in the 298–773 K temperature range.

4. Results and discussion

4.1. Characterization of Rh/CeO_2 LS and Rh/CeO_2 HS

For Rh/CeO_2 LS, benzene hydrogenation permitted to estimate that 18.6% of the total rhodium loading was zero-valent and accessible, corresponding to Rh(0) particles of about 4.5 nm in size. No Rh^{x+} could be detected by NO titration.

In the case of Rh/CeO_2 HS only 20% of the rhodium content was accessible as zero-valent atoms over the high ceria surface area sample. Complementary we verified by NO titration, that 80% of the rhodium loading was stabilized into cerium vacancies of the support as Rh^{x+} and accessible to NO on the surface of the reduced Rh/CeO_2 HS sample.

4.2. $CO/NO/O_2$ reactions over Rh(0) active sites (Rh/CeO_2 LS catalyst) during TPSR

Fig. 1 reports reactant (NO, CO) concentrations measured continuously by selective detectors at the outlet of the reactor, during temperature-programmed surface reactions. The upper part of the plot (line 'zero conversion') corresponds to the initial concentrations of reactants. Above this level all desorption will appear as a positive signal. Under this zero-level, consumptions of reactants take place for conversion higher than zero. Temperatures of light-off are not so much indicative of turnover rates of reactions, as they depend on the number and quality of active sites.

Rh/CeO_2 LS only presents Rh(0) active sites. Let us note that no desorption peaks appear during the whole reaction (Fig. 1), on the contrary of what

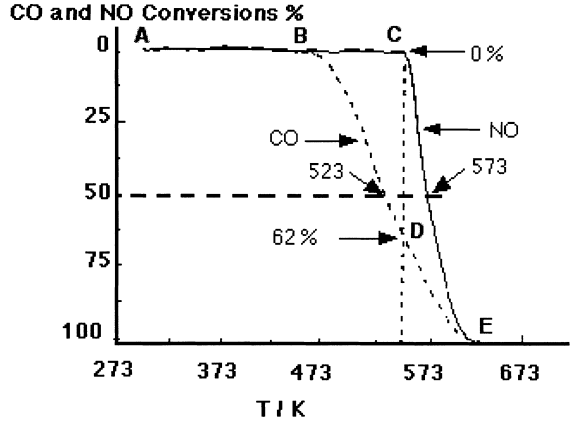

Fig. 1. CO and NO conversion curves in the 298–773 K temperature range over the low surface area Rh/CeO_2 LS sample pretreated at 773 K in hydrogen. Gas mixture: 1.5 vol.% CO, 0.20 vol.% NO, 0.65 vol.% O_2 in He; feed stream: 15 l h^{-1}; heating rate: 453 K h^{-1}; catalyst weight: 200 mg.

happens on Rh($^{x+}$) catalysts (Fig. 4, point C). It means that NO does not adsorb at low temperature, or if it adsorbs, it decomposes leaving adsorbed oxygen atoms (*O) on the surface of Rh(0). Once the surface is saturated by *O (from NO or dioxygen of the reaction mixture), NO has no more any possibility of dissociative adsorption over Rh(0). This is the reason why NO does not react before 543 K (Fig. 1, point C).

Furthermore, catalytic cycles in Fig. 2 are designed to represent the events observed during the TPSR reported in Fig. 1. For a better understanding of the methodology to designing the 2 catalytic cycles (Fig. 2), let us recall that for a stoichiometric mixture $CO/NO/O_2$, 86.7 mol% CO are oxidized to CO_2 by the total number of adsorbed oxygen atoms provided by dioxygen of the reaction mixture. The remaining 13.3 mol% CO will be oxidized by *O provided by the decomposition of NO: it results in the simultaneous 100% conversions of both CO and NO at E (Figs.1–2, point E).

Let us recall that the experimental device for $CO/NO/O_2$ reaction is equivalent to a CSTR reactor: it means that the composition of the outlet gases is such that it represents the composition of the gas mixture in contact with the catalyst. So when all dioxygen has been consumed to oxidize CO to CO_2, it corresponds on Fig. 1 to 86.7 mol% CO transformed to CO_2.

From point A to point B (Fig. 1), no CO nor NO are consumed. At point B (Fig. 1), CO begins to oxidize to CO_2, whereas NO is still not consumed till point C (Fig. 1). It means that NO cannot access the catalytic active sites, so the cycle CO/NO (Fig. 2) still do not turnover, whereas CO and O_2 adsorb and react to give CO_2 (cycle CO/O_2, Fig. 2). The point C (Fig. 1) corresponds to 62% conversion of CO by O_2 alone, as NO remains constant in the gas phase. At that temperature (Figs. 1–2, point C or D), NO begins to react: it adsorbs and decomposes over Rh(0), as previously considered in the above sections. It means that NO can now adsorb, probably due to the high reactivity between CO and *O from O_2, leaving free metallic sites accessible to NO. So at point D (Fig. 1) CO both consumes *O from flowing O_2 and NO: this is the coupling point of cycles CO/NO and CO/O_2, (Fig. 2). In this transient experiment, when all oxygen atoms from O_2 have been consumed by CO to CO_2, corresponding to 86.7% CO conversion to CO_2, it can be observed that CO still continue to be oxidized and can be totally transformed to CO_2: as NO also goes toward total conversion after 86.7% CO conversion, it means that both CO and NO react according to the 2 cycles CO/O_2 and CO/NO in the flowing mixture of the CSTR reactor (Fig. 2) and as a consequence they simultaneously get the point E (Fig. 1) where both 100% CO and NO conversions are observed.

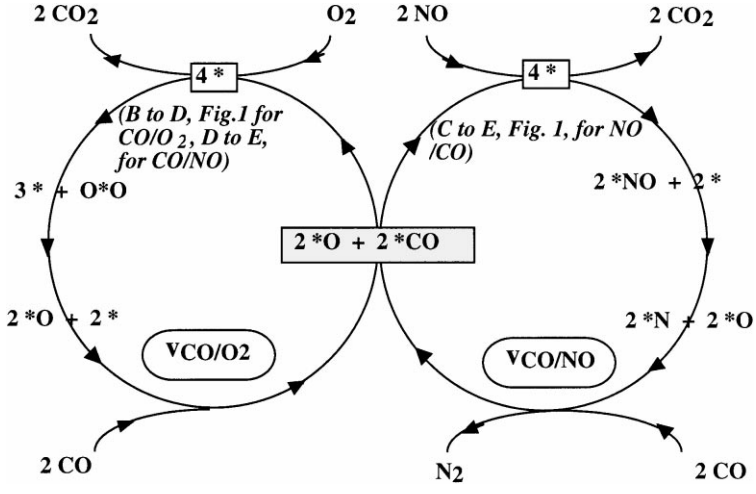

Fig. 2. Catalytic cycles for the $CO/NO/O_2$ reactions (dissociative mechanism) over Rh(0) active sites on Rh/CeO_2 LS.

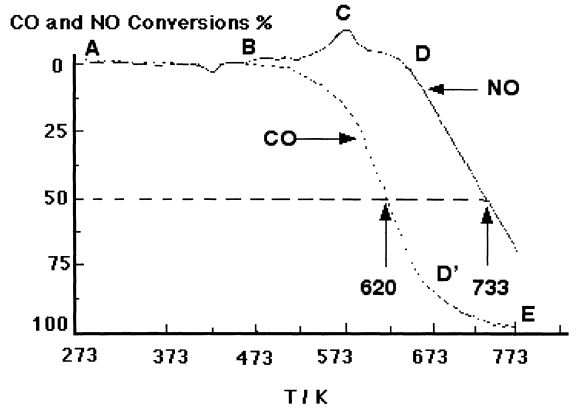

Fig. 3. CO and NO conversion curves in the 298–773 K temperature range over the high surface area ceria support pretreated at 773 K in hydrogen. Gas mixture: 1.5 vol.% CO, 0.20 vol.% NO, O.65 vol.% O_2 in He; feed stream: $l5lh^{-1}$; heating rate: $453 K h^{-1}$; catalyst weight: 200 mg.

All these events are summarized by the coupling of the two catalytic cycles as shown in Fig. 2. The cycle on the left corresponds to the Route 4 (Table 1) and to the unique CO oxidation by $^*O$ (Route 2, Table 1). As the selectivity of reaction for N_2 was near 100% Route 4 does not consider steps 9 and 10. $^*O$ species is only due to dioxygen of the reaction mixture for a temperature less than 543 K (Fig. 1, point C or D). At 543 K the right cycle begins to turnover, corresponding to the NO adsorption, decomposition and reduction to N_2, assisted by CO oxidation as observed in Fig. 1 (Route 1, Table 1). CO consumes $^*O$ left by NO dissociation. Left and right cycles have to be coupled by a common point corresponding to a surface partially occupied by $^*O$ produced by both O_2 and NO dissociations and $^*CO$ (adsorbed CO). So, $^*O$ can originate from both left and right cycles: this is the origin of the kinetic coupling of the two cycles [31]. These two cycles, according to the Quasi-Stationary State Approximation, do not turnover with the same rate [31]. All features given in the literature can be found in this model.

In conclusion, Fig. 2 only reports elementary steps as deduced from the global data obtained from the TPSR in Fig. 1. Fig. 2 mainly deals with NO decomposition and N_2 desorption, (no N_2O was observed over the actual catalyst) and CO oxidation by $^*O$ from O_2 or NO, as far as the NO/CO cycle has begin to turnover, that is for a temperature higher than 473 K. (Fig. 1, point C).

4.3. CO / NO / O_2 reactions over cationic sites during TPSR

Figs. 3 and 4 report the $CO/NO/O_2$ reactions over Ce^{3+} and Rh^{x+} (considered to be Rh^+ in Fig. 6), respectively.

Fig. 3 shows that the support alone is able to proceed to the $CO/NO/O_2$ reactions. Both figures present the same features, but Ce^{3+} is less active than Rh^{x+} which is able to catalyze the reaction at 473 K compared to approximately 573 K for ceria alone.

Furthermore, even at 773 K, ceria is not able to give 100% conversion of CO and NO. TPSR over ceria will be first described and a more detailed analysis of Rh/CeO_2 will be given, in order to better design the catalytic cycle reported in Fig. 6.

$CO/NO/O_2$ reactions over $(_V)$-Ce^{3+}-$(_V)$. Fig. 3 reports the plots obtained over bare ceria. First of all, according to Soria data, it appears that bare ceria is able to proceed to the $CO/NO/O_2$ reactions in a way which globally looks like that observed over Rh(0). The oxidation of CO first begins to occur at about 473 K, but simultaneously NO is activated and desorbing, leaving the surface for the CO/O_2 reac-

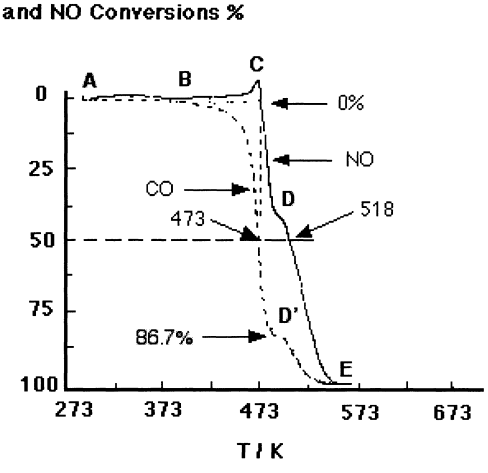

Fig. 4. CO and NO conversion curves in the 298–773 K temperature range over the high surface area Rh/CeO_2 HS sample pretreated at 773 K in hydrogen. Gas mixture: 1.5 vol.% CO, 0.2 vol.% NO, 0.65 vol.% O_2 in He; feed stream: $l5lh^{-1}$; heating rate: $453 K h^{-1}$; catalyst weight: 200 mg.

tion to occur on the active sites. This is the major difference compare to the process over Rh(0). The temperature of light-off of CO is quite higher than that over Rh(0) — 620 K instead of 523 K — and subsequently at 620 K, NO have access to the surface and begin to decompose and to reduce to N_2. Again the temperature of light-off of NO is quite higher: 733 K instead of 573 K over Rh(0). Before looking for the catalytic sequence occurring in the presence of cationic sites, let us consider data over Rh/CeO_2 HS.

4.3.1. $CO/NO/O_2$ reactions over Rh/CeO_2 HS

This material only presented accessible Rh^{x+} active sites (Fig. 4). These sites can be produced by pretreating the material by the $CO/NO/O_2$ flowing mixture, up to 700 K [14]. Fig. 5, step 1, reports a scheme for the active site, where the support has been reduced during the pretreatment: Rh^{x+} has 2 oxygen vacancies in its neighboring, as also designed in the catalytic cycle in Fig. 6.

At room temperature (Fig. 4, point A), NO must chemisorb without any dissociation, as it is found to desorb as NO between points B and C (Fig. 4). So, from curve A to B, neither CO nor NO, are globally consumed, but the surface is covered by NO, as shown step 2, Fig. 5. At about 380 K (Fig. 4, point B), CO is seen to begin to oxidize to CO_2, whereas the non-dissociatively pre-adsorbed NO at room temperature, is found to desorb, leaving the surface for the CO/O_2 reaction to occur (Fig. 4, from point B to point C).

At about 475 K, there is almost 60% CO conversion, and at D′ when CO conversion is 86% (complete dioxygen consumption), NO is observed to react, as seen in the outlet gas phase (which is the same on the catalyst of the CSTR reactor used). It means that, as in the case of Rh(0), once CO has consumed all the dioxygen of the flowing reaction mixture to give CO_2, some of the active sites begin to be free and NO adsorbs again as dinitrosyl or dinitrosyl species (step 2, Fig. 5, or $(NO)_2$ adsorbed species in the catalytic cycle, Fig. 6). The same NO: $Rh^{x+} = 2$ stoichiometry is assumed, as found over Rh/CeO_2–ZrO_2 [14]. It is clear that above about 480 K (Fig. 4, point D′), both CO and NO are found to react simultaneously. Step 3 (Fig. 5) shows that 2CO can adsorb on Rh^{x+} as two strong ligands, whereas N_2O must form to justify its detection at a

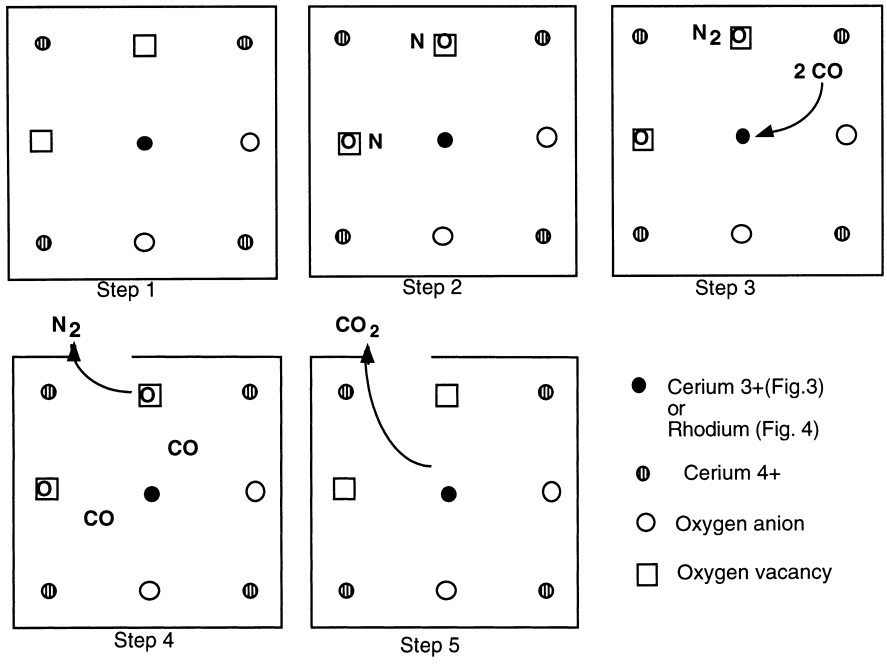

Fig. 5. Molecular schemes for elementary steps as deduced from Figs. 3 and 4.

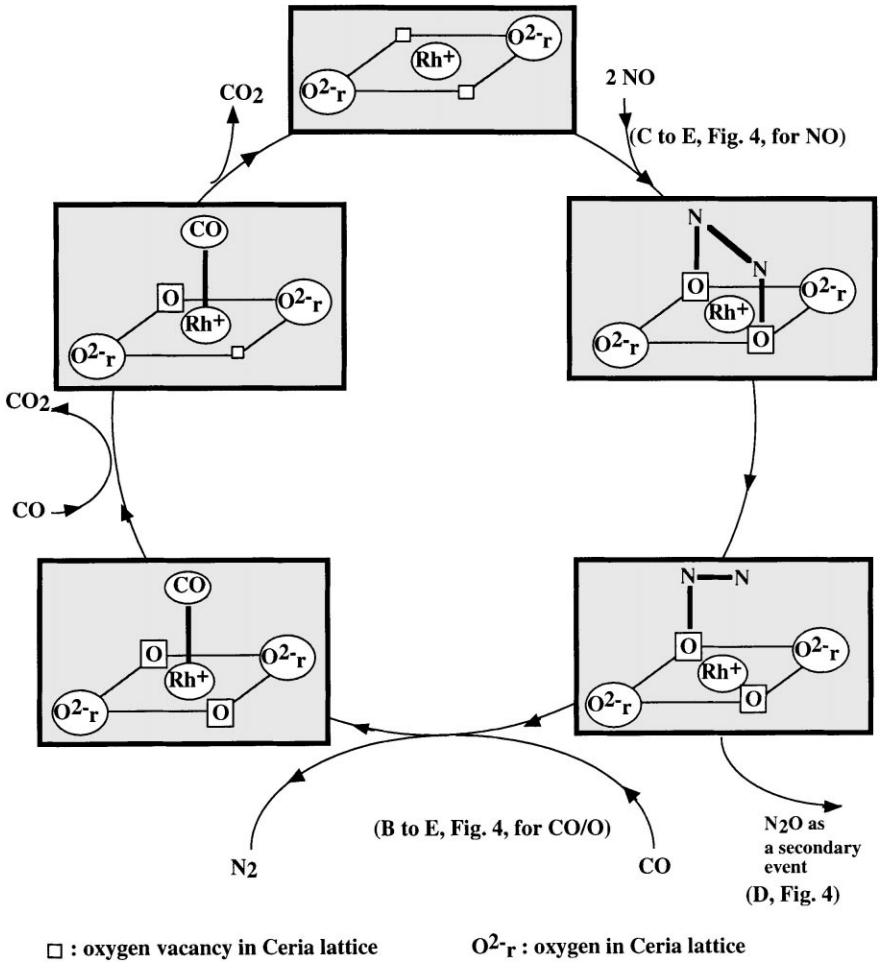

Fig. 6. Catalytic cycle for the CO/NO reactions (associative mechanism) over ($_V$)-Rh^+-($_V$) mixed site on Rh/CeO_2 HS.

very low concentration in the outlet gas phase during the TPSR (transient production of N_2O at D′). It corresponds to one N–O bond breaking, as proposed in the cycle in Fig. 6. As NO selectively transforms to N_2 (point C to point E), step 4 (Fig. 5) corresponds to 2^*O and 2^*CO in the coordinative sphere of Rh^{x+} which can lead to the production of CO_2 (Fig. 4, point D′ to point E; CO adsorption and CO_2 desorption steps in the cycle (Fig. 6)), regenerating the active sites. Figs. 5 and 6 are no more than corresponding to the process observed between point C and point D on the TPSR plot in Fig. 4.

Fig. 6 reports a catalytic cycle were Ce^{3+} could substitute Rh^+ in the case of bare ceria. Globally it can be considered as a supported homogeneous catalytic system.

For a sake of simplicity, it only shows the CO/NO reactions and does not take into account the CO/O_2 reaction. It corresponds to the NO associative chemisorption to produce a dinitrosyl species which, in a first step begins to suffer a N–O bond scission (which can lead to a weak N_2O desorption for a bad catalyst); a second N–O bond scission leads to N_2 and leaves two oxygen species adsorbed in the coordinative sphere of Rh^+. Then CO adsorbs to clean the site from these two oxygen species, which could inhibite a further adsorption of new NO molecules. These oxygen species could be also produced from dioxygen.

In conclusion, taking into account data from literature and the theoritical basis of the model (Section 2), all events detected in TPSR (Fig. 1 and Figs.

3–4) can be summarized in the schemes reported Fig. 5. From these schemes and using the set of elementary steps (Table 1) associated with their stoichiometric number, it is easy to design catalytic sequences as cycles. Comparing the two kinds of catalytic cycles (Figs. 2 and 6), it can be said that we have the same global events but on different active sites.

1. NO decomposition.
2. Oxygen-scavenging by CO to clean the active site, avoiding the inhibiting effect of oxygen species for a further NO chemisorption.

The very beauty of these catalytic processes is the 'assisted' aspect of the two reactions, resulting in their kinetic coupling. Fig. 2 clearly shows that CO reacts with adsorbed oxygen atoms provided by both O_2 and NO of the feed. In both cases (Figs. 2 and 6), CO is first oxidized, then NO dissociates when the surface becomes accessible. Cycles presented Figs. 2 and 6 turnover at a temperature where NO is activated.

In the next paper, we shall discuss the deNO_x reactions: that is the 'reduction' of NO in the presence of a hydrocarbon, in an excess of dioxygen. From all these discussions, the design of the 'best and stable' catalyst would be deduced. Combination analysis would be very helpful for optimizing these concerted reactions.

Acknowledgements

The authors greatly acknowledge Professor Michel Boudart for fruitful discussions.

References

[1] V.I. Pârvulescu, P. Grange, B. Delmon, Catal. Today 46 (1998) 233.
[2] R. Burch, P.J. Millington, Appl. Catal. B: Environ. 2 (1993) 101.
[3] T.P. Kobylinski, B.W. Taylor, J. Catal. 33 (1974) 376.
[4] H. Arai, H. Tominaga, J. Catal. 43 (1976) 131.
[5] C.T. Campbell, J.M. White, Appl. Surface Sci. 1 (1978) 347.
[6] T.N. Root, L.D. Schmidt, G.B. Fisher, Surface Sci. 150 (1985) 173.
[7] K.C. Taylor, J.C. Schlatter, J. Catal. 63 (1980) 53.
[8] S.H. Oh, G.B. Fisher, J.E. Carpenter, D.W. Goodman, J. Catal. 100 (1986) 360.
[9] B.K. Cho, B.H. Shanks, J.E. Bailey, J. Catal. 115 (1989) 486.
[10] E.A. Hyde, R. Rudham, C.H. Rochester, J. Chem. Soc., Faraday Trans. 1 80 (1984) 531.
[11] R. Krishnamurthy, S.S.C. Chuang, M.W. Bakalos, J. Catal. 157 (1995) 512.
[12] R. Krishnamurthy, S.S.C. Chuang, J. Phys. Chem. 99 (1995) 16727.
[13] S.S.C. Chuang, R. Krishnamurthy, C.-B. Tan, Colloids Surfaces A: Physicochem. Eng. Aspects 105 (1995) 35.
[14] F. Fajardie, J.-F. Tempère, J.-M. Manoli, O. Touret, G. Blanchard, G. Djéga-Mariadassou, J. Catal. 179 (1998) 469.
[15] R. Burch, P.J. Millington, A.P. Walker, Appl. Catal. B: Environ. 4 (1994) 65.
[16] G. Leclercq, C. Dathy, G. Mabilon, L. Leclercq, in: A. Crucq (Ed.), Catalysis and Automotive Pollution Control II, 1991, p. 181.
[17] J. Kaspar, C. de Leitenburg, P. Fornasiero, A. Trovarelli, M. Graziani, J. Catal. 146 (1994) 136.
[18] W.C. Hecker, A.T. Bell, J. Catal. 84 (1983) 200.
[19] T.R. Ward, R. Hoffman, M. Shelef, Surface Sci. 289 (1993) 85.
[20] M. Primet, J.C. Vedrine, C. Naccache, J. Mol. Catal. 4 (1978) 411.
[21] D.G. Castner, G.A. Somorjai, Surface Sci. 83 (1979) 60.
[22] T. Iiuzuka, J.H. Lunsford, J. Mol. Catal. 8 (1980) 391.
[23] D.E. Hendriksen, C.D. Meyer, R. Eisenberg, Inorg. Chem. 16 (1977) 970.
[24] L. Salin, Ph.D Thesis, Pierre et Marie Curie University, 1997.
[25] F. Fajardie, J.-F. Tempère, G. Djéga-Mariadassou, G. Blanchard, J. Catal. 163 (1996) 77.
[26] A. Martinez-Arias, J. Soria, J.C. Conesa, X.L. Seoane, A. Arcoya, R. Cataluna, J. Chem. Soc., Faraday Trans. 91 (11) (1995) 1679.
[27] R. Cataluna, A. Arcoya, X.L. Scoane, A. Martinez-Arias, J.M. Coronado, J.C. Conesa, J. Soria, L.A. Petrov, in: A. Frennet, J.M. Bastin (Eds.), Catalysis and Automotive Pollution Control III, Studies in Surface Science and Catalysis 96 (1995) 215.
[28] M. Primet, J. Chem. Soc., Faraday Trans. 1 74 (1978) 2570.
[29] B. Harrison, A.F. Diwel, C. Hallett, Platinum Metal Rev. 32 (1988) 73.
[30] R. Burch, P.J. Millington, A.P. Walker, Appl. Catal. B 4 (1994) 65.
[31] M. Boudart, G. Djéga-Mariadassou, Kinetics of Heterogeneous Catalytic Reactions, Princeton University. Press, Princeton, NJ, 1984 (in French), Masson, Paris, 1982.
[32] L. Salin, C. Potvin, J.-F. Tempère, M. Boudart, G. Djéga-Mariadassou, J.M. Bart, Ind. Eng. Res. 37 (1998) 4531.